A new approach to retrieving cirrus cloud height with a combination of MODIS 1.24- and 1.38-μm channels

Chenxi Wang,[1] Shouguo Ding,[1] Ping Yang,[1] Bryan Baum,[2] and Andrew E. Dessler[1]

[1]   An approach is developed for inferring cloud top height (CTH) by using two shortwave infrared (SWIR) channels (i.e., 1.24- and 1.38-μm) with similar cloud scattering and absorption properties but very different water vapor absorption properties. This channel combination is used to accurately infer the column water vapor amount above the clouds, from which the CTH can be retrieved. The approach performs best for ice clouds located in the upper troposphere. For those clouds, our approach performs as well or better than the current operational cloud height retrieval algorithm adopted by the MODIS science team. **Citation:** Wang, C., S. Ding, P. Yang, B. Baum, and A. E. Dessler (2012), A new approach to retrieving cirrus cloud height with a combination of MODIS 1.24- and 1.38-μm channels, *Geophys. Res. Lett.*, *39*, L24806, doi:10.1029/2012GL053854.

1.   Introduction

[2]   The CO_2 slicing algorithm [*Menzel et al.*, 1983; *Wylie and Menzel*, 1999] is widely used to retrieve cloud top pressure (CTP) from numerous instruments such as the MODerate resolution Imaging Spectroradiometer (MODIS) [*Platnick et al.*, 2003] and the High resolution Infrared Radiometer Sounder (HIRS) [*Wylie and Menzel*, 1999]. The method is sensitive to middle and high-level clouds, and provides robust retrievals during both daytime and nighttime [*Menzel et al.*, 2010]. However, *Holz et al.* [2008] found that MODIS Collection 5 (C5) mean cloud top heights were frequently lower than collocated Cloud-Aerosol Lidar with Orthogonal Polarization (CALIOP) measurements. By investigating the spatial distribution of the CTH differences, *Holz et al.* [2008] found that the biggest differences occurred in the Inter-Tropical Convergence Zone (ITCZ), where thin cirrus clouds frequently occur due to both deep convection [*Jensen et al.*, 1996; *Rosenfield et al.*, 1998; *Wang and Dessler*, 2012] and radiative cooling [*Garrett et al.*, 2006; *Wang and Dessler*, 2012].

[3]   The CO_2 slicing algorithm retrieves a radiative effective height (i.e., an effective height satisfying a cloud pressure function defined by *Smith and Platt* [1978, equation (1)], which is located at a geometrical depth within the cloud (beginning at cloud top) where the integrated optical thickness is about 1 [*Holz et al.*, 2006]. Figure 1 shows the scaled frequency of ΔCTH (CALIOP − MODIS C5) as a function of CALIOP cloud optical thickness (τ_{CALIOP}). The scaling factor is the highest value of the frequency in each τ_{CALIOP} bin; the CALIOP–detected multi-layered cloud pixels are removed from consideration. For most of the cases, CALIOP and MODIS CTH values are consistent with each other, with ΔCTH values limited to $\pm$1km. However, for $\tau_{CALIOP} < 0.7$, the absolute values of ΔCTH clearly increase, suggesting that, in comparison with observations of CALIOP, the MODIS CTH is more variable at these low optical thickness values, and may even fail to retrieve a cloud height for some cases as evidenced by the maximum ΔCTH frequency bin in the upper left corner of Figure 1. The relatively large ΔCTH indicates that, if a cloud is optically thin, the application of the CO_2 slicing algorithm becomes problematic due to the relatively weak cloud signal-to-noise ratio in the thermal infrared CO_2 absorption channels [*Menzel et al.*, 2010]. The surface and lower atmosphere contribute more emission to the satellite-received signal and, therefore, increase the retrieval uncertainty. Another possible reason for the large CTH bias between MODIS C5 and CALIOP is an error in the knowledge of the positions of spectral response functions of MODIS CO_2 bands [*Tobin et al.*, 2006]. This effect may be mitigated by slightly shifting the spectral response functions, as suggested by *Tobin et al.* [2006] and *Baum et al.* [2012]. Although effective radiating heights are useful and convenient for some atmospheric problems, physical cloud heights are sometimes more important — e.g., for studying the formation of thin cirrus clouds [*Sassen et al.*, 2009] and the latent heat release associated with phase changes [*Corti et al.*, 2006].

[4]   In comparison with the IR bands, the 1.38-μm channel measures the reflection of clouds above the level where water vapor attenuates the signal, and is particularly useful for studying high clouds. The strong water vapor (WV) absorption in this channel prohibits photons from reaching the lower troposphere, substantially increasing the sensitivity to thin cirrus clouds located in the upper troposphere. This characteristic of the 1.38-μm channel, different from other shortwave infrared (SWIR) channels, is advantageous for studying the optical properties of thin cirrus clouds [*Gao et al.*, 1998, 2002, 2004; *Dessler and Yang*, 2003; *Meyer et al.*, 2004; *Meyer and Platnick*, 2010]. In this paper, we develop a new CTH retrieval approach based on two SWIR channels (i.e., 1.24- and 1.38-μm).

2.   Method

[5]   The solar reflectance received by the satellite from a single-layer cirrus cloud can be expressed as the summation

---

[1]Department of Atmospheric Sciences, Texas A&M University, College Station, Texas, USA.

[2]Space Science and Engineering Center, University of Wisconsin-Madison, Madison, Wisconsin, USA.

Corresponding author: P. Yang, Department of Atmospheric Sciences, Texas A&M University, College Station, TX 77843, USA. (pyang@tamu.edu)
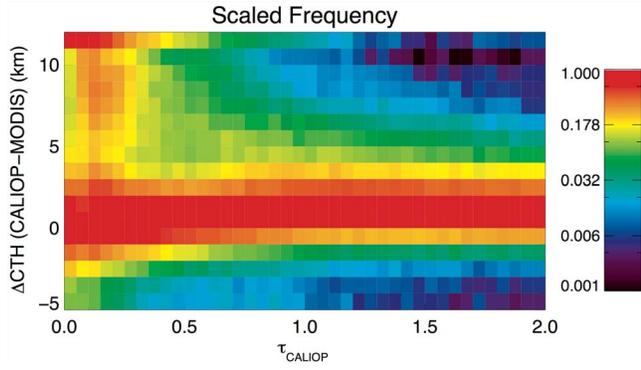
Figure 1. Frequency of ΔCTH (CALIOP − MODIS) as a function of τ_{CALIOP}. The frequency is scaled by dividing the largest frequency in each τ_{CALIOP} bin. Data are from collocated MODIS and CALIOP measurements made in August 2006.

of two parts [*Gao et al.*, 2002; *Meyer and Platnick*, 2010]:

$$R_{obs,\lambda} = R_{c,\lambda}\left(\tau_c, D_{eff}, \mu, \phi, -\mu_0, \phi_0\right) T_{two-way,\lambda}\left(\tau_{g,\lambda}, \mu, -\mu_0\right)$$
$$+ b_\lambda\left(\tau_c, D_{eff}, \mu, \phi, -\mu_0, \phi_0, r_s\right), \tag{1}$$

where $R_{obs,\lambda}$ is the satellite-observed reflectance, $R_{c,\lambda}$ is the cirrus cloud reflectance, $T_{two-way,\lambda}$ is the two-way transmittance including the effects from gas absorption and Rayleigh-scattering above (and within) the cloud layer, b_λ is the reflectance associated with lower level gases and the surface, ϕ is the satellite azimuth angle, μ is the cosine of the satellite viewing zenith angle, ϕ_0 and μ_0 indicate the corresponding geometry of the sun, λ is the wavelength, τ_c and D_{eff} are the visible optical thickness and effective particle diameter of a cirrus cloud, $\tau_{g,\lambda}$ is the gas optical thickness, and r_s is surface bi-directional reflection. The goal of this CTH retrieval method is to derive either $T_{two-way}$ or τ_g in the 1.38-μm channel with a combination of a solar reflectance channel (e.g., 0.86-, 1.24-, or 1.64-μm channel) and the 1.38-μm channel.

[6] For a window channel, equation (1) reduces to:

$$R_{obs,window} = R_{c,window}\left(\tau_c, D_{eff}, \mu, \phi, -\mu_0, \phi_0\right)$$
$$+ b_{window}\left(\tau_c, D_{eff}, \mu, \phi, -\mu_0, \phi_0, r_s\right), \tag{2}$$

because $T_{two-way,window}$ is close to 1. For the 1.38-μm channel, the reflectance can be expressed as [*Meyer and Platnick*, 2010]:

$$R_{obs,1.38} = R_{c,1.38}\left(\tau_c, D_{eff}, \mu, \phi, -\mu_0, \phi_0\right)$$
$$T_{two-way,1.38}\left(\tau_{g,1.38}, \mu, -\mu_0\right), \tag{3}$$

where $b_{1.38}$ vanishes due to strong WV absorption. More assumptions are needed to derive $T_{two-way,1.38}$ from equations (2) and (3). *Gao et al.* [1998] found a linear relationship between window channel cloud reflectance ($R_{c,\lambda}$, $0.4 < \lambda < 1.0~\mu$m) and $R_{c,1.38}$. *Meyer and Platnick* [2010] found the ratio of $R_{c,1.24}$ to $R_{c,1.38}$ to be approximately independent of D_{eff} because ice crystal scattering properties are similar in these two channels.

[7] Based on these previous studies, we can describe the ratio of $R_{c,1.24}$ to $R_{c,1.38}$ as a function of solar-satellite geometry:

$$\Gamma(\mu, \phi, -\mu_0, \phi_0) = R_{c,1.24}/R_{c,1.38}, \tag{4}$$

In this study, to determine Γ, we use the rigorous Discrete Ordinates Radiative Transfer model (DISORT) [*Stamnes et al.*, 1988] in a 128-stream mode to generate a lookup table of $\Gamma(\mu, \phi; -\mu_0, \phi_0)$. The incoming and outgoing directions are defined on the normal directions of 160 facets of a twisted icosahedral mesh [*Heikes and Randall*, 1995]. As such, a 160×160 matrix of Γ is pre-computed and whose rows and columns represent incident and viewing directions. For a given solar-satellite geometry, 35 τ_c values from 0.1 to 10.0 and 18 D_{eff} values from 10 to 180 μm are selected to build computed $R_{c,1.24}$ and $R_{c,1.38}$ pairs (630 pairs for each geometry). Γ is statistically calculated with linear regression. For simplification, only the direct reflection (i.e., first order of surface reflection) is considered to derive the $b_{1.24}$ as follows:

$$b_{1.24} = \exp\left(-\frac{\tau_c}{\mu}\right)\exp\left(-\frac{\tau_c}{\mu_0}\right)r_s. \tag{5}$$

The gas absorption in the 1.24-μm is totally ignored since the gas optical thickness of the entire atmosphere has a magnitude of 0.02 (i.e., calculated using the U.S. Standard atmospheric profile [*Anderson et al.*, 1986]). The two-way transmittance in the 1.38-μm channel can be derived from equation (2)–(5) as:

$$T_{two-way,1.38} = \frac{R_{obs,1.38} \times \Gamma(\mu, \phi, -\mu_0, \phi_0)}{R_{obs,1.24} - b_{1.24}}. \tag{6}$$

$\tau_{g,1.38}$ can be derived from the two-way transmittance and the solar-satellite geometry as follows:

$$\tau_{g,1.38} = -\frac{\mu_0 \mu}{(\mu_0 + \mu)}\ln(T_{two-way,1.38}). \tag{7}$$

[8] The surface bi-directional reflectance, r_s, is simulated with the Cox-Munk model for an ocean surface [*Cox and Munk*, 1954] and over land using an MODIS operational albedo model [*Schaaf et al*, 2002]. The cloud optical thickness, τ_c, is extracted from the MODIS Collection 5 product. The surface term $b_{1.24}$ is related to τ_c, r_s and the accuracy of first order reflection shown in equation (5). The derived $T_{two-way,1.38}$, however, is insensitive to $b_{1.24}$ because $b_{1.24}$ is one or two orders of magnitude smaller than $R_{obs,1.24}$ under normal conditions (e.g., non-sunglint pixels). We will further discuss the retrieval sensitivity on $b_{1.24}$ in Section 4. Consequently, CTH is inferred using an interpolation method with the corresponding column absorbing gas optical thickness profile, which is obtained using the correlated-k distribution method (S. Ding et al., Development of a GOES-R Advanced Baseline Imager solar channel radiance simulator for ice clouds, submitted to *Journal of Applied Meteorology and Climatology*, 2012) and atmospheric profile from the Modern Era Retrospective-analysis for Research and Application (MERRA) [*Rienecker et al.*, 2008] reanalysis data.

3. Case Study

[9] Figure 2a shows an Aqua MODIS 1.24-μm reflectance granule gray scale image collected on 12 September 2008.
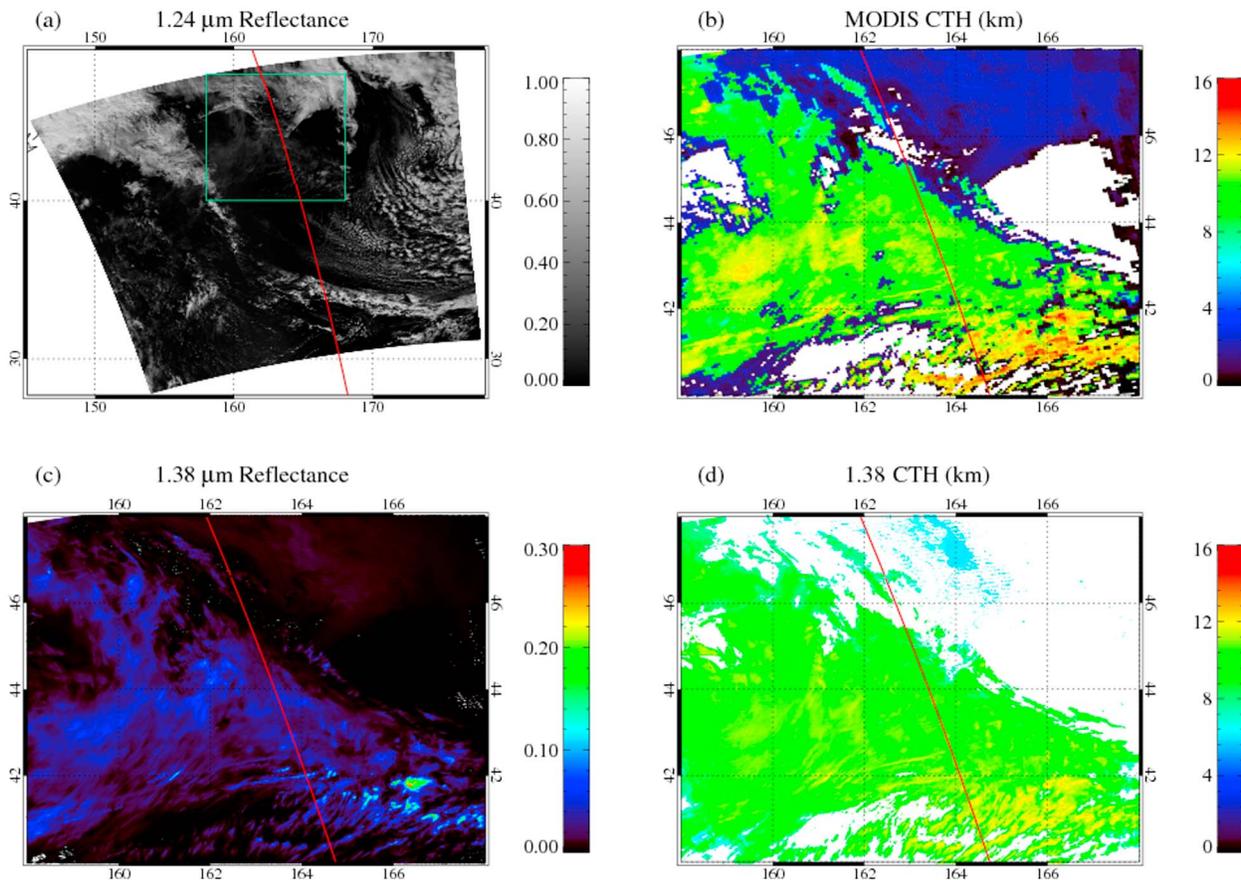
Figure 2. A case study of the 1.38 CTH retrieval method (0215) UTC, 12 September 2008. (a) Gray scale image of MODIS 1.24-μm channel reflectance. The region of interest is outlined with the green box. The red line indicates the corresponding CALIPSO track. (b) MODIS retrieved CTH. (c) MODIS 1.38-μm channel reflectance. (d) CTH retrieved using the 1.38-μm method.

The region of interest (ROI) is located in the northern Pacific Ocean and is outlined with the green box. The red line indicates the CALIPSO (Cloud-Aerosol Lidar and Infrared Pathfinder Satellite Observation) track. Optically thin cirrus cloud can be recognized around the lower part in the green box. Figure 2c shows the MODIS 1.38-μm reflectance in the ROI. As expected, this channel highlights high clouds but the strong WV absorption masks the detection of low clouds. Figures 2b and 2d show MODIS retrieved CTHs and the 1.38-μm channel based CTHs (hereafter referred to as 1.38 CTH), respectively. The Collection 5 MODIS product provides the CTP with a 5 km spatial resolution and the corresponding CTH value is derived using ancillary data extracted from the MERRA data. Although based on the same cloud mask product (i.e., from the MODIS Collection 5), the new method provides more extensive coverage of thin cirrus CTH than its MODIS counterpart.

[10] As shown in Figure 3a, we compare the 1.38, MODIS, and CALIOP CTHs along the CALIPSO track to validate the 1.38 CTH. Generally, the 1.38 CTH values are consistent and located between the CALIOP cloud physical boundaries. Between 40.3° to 40.6°N and 44.6° to 45.0°N, the physical structures of the clouds become complicated and the 1.38 CTH can be influenced by the three dimensionality of clouds, the presence of multilayered clouds, and more.

[11] The relatively large variations in MODIS CTH values suggest that inferring CTH is problematic for very optically thin clouds. For instance, the MODIS and CALIOP CTH values are quite close if the cloud is opaque (e.g., 42.5° to 43.0°N and 43.5° to 44.2°N) and the MODIS τ_c values are larger than 2. However, if the cloud is optically thin, then the MODIS CTH values tend to either underestimate the true CTH (e.g., 42.2° to 42.5°N and 44.7° to 45.4°N), perhaps due to a slight overestimation of cloud effective emissivity [*Menzel et al.*, 2010], or miss cirrus clouds (e.g., 40.2° to 40.8°N,) perhaps due to relatively large uncertainties in the surface and other ancillary data or due to low signal-to-noise in the measurements.

[12] In contrast, the 1.38 CTH retrieval method is independent of temperature profile, surface temperature and emissivity, and the amount of WV and other gases in the lower atmosphere. Furthermore, the dependence on cloud microphysical and optical properties is not a factor with the use of the 1.24 to 1.38-μm reflectance ratio.

4. Discussion

[13] The accuracy of the 1.38 CTH retrieval is closely related to the accuracy of the WV concentration and the surface term $b_{1.24}$. Figure 4 shows their influences on the 1.38 CTH retrieval. Three typical atmospheric profiles (i.e., US standard, tropical, and subarctic winter [*Anderson et al.*, 1986]) are used to conduct the error analysis. Figure 4a
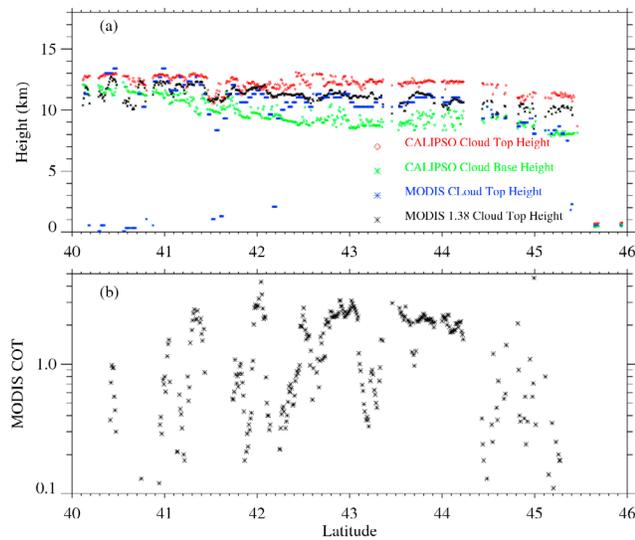
Figure 3. (a) Comparison between CALIOP, MODIS, and 1.38 CTH values along the CALIPSO track shown in Figure 2. (b) Corresponding MODIS cloud optical thickness values.

shows the cumulative WV optical thickness values (from cloud top to the top of atmosphere) as a function of the CTH (solid lines). The sensitivity is depicted in Figure 4a using dotted lines (+10% WV concentration errors) and dashed lines (−10% errors). For a given WV cumulative optical thickness derived from 1.24- and 1.38-μm observations, an overestimation of the WV amount (e.g., due to errors in the MERRA data) will increase the CTH and an underestimation of the WV amount will lower the CTH. Figure 4b shows the errors of the 1.38 CTH caused by uncertainties in the WV amount as a function of the CTH. Relatively large errors (0.8 km and 0.4 km for 20% and 10% WV errors) can be found in dry atmospheres (e.g., subarctic winter profile). In humid conditions (e.g., tropical profile), however, errors are minimized because τ_g is large enough and therefore can be retrieved correctly. Moreover, large errors can be found for high clouds (i.e., CTH ≈ 14 km for humid conditions and CTH ≈ 12 km for dry conditions) because the WV amount is quite small above 12 km. For this reason, a slight change in WV profile significantly impacts the 1.38 CTH. As the CTH decreases (9 km < CTH < 12 km, the error decreases because the cumulative WV optical thickness is rapidly increasing. The
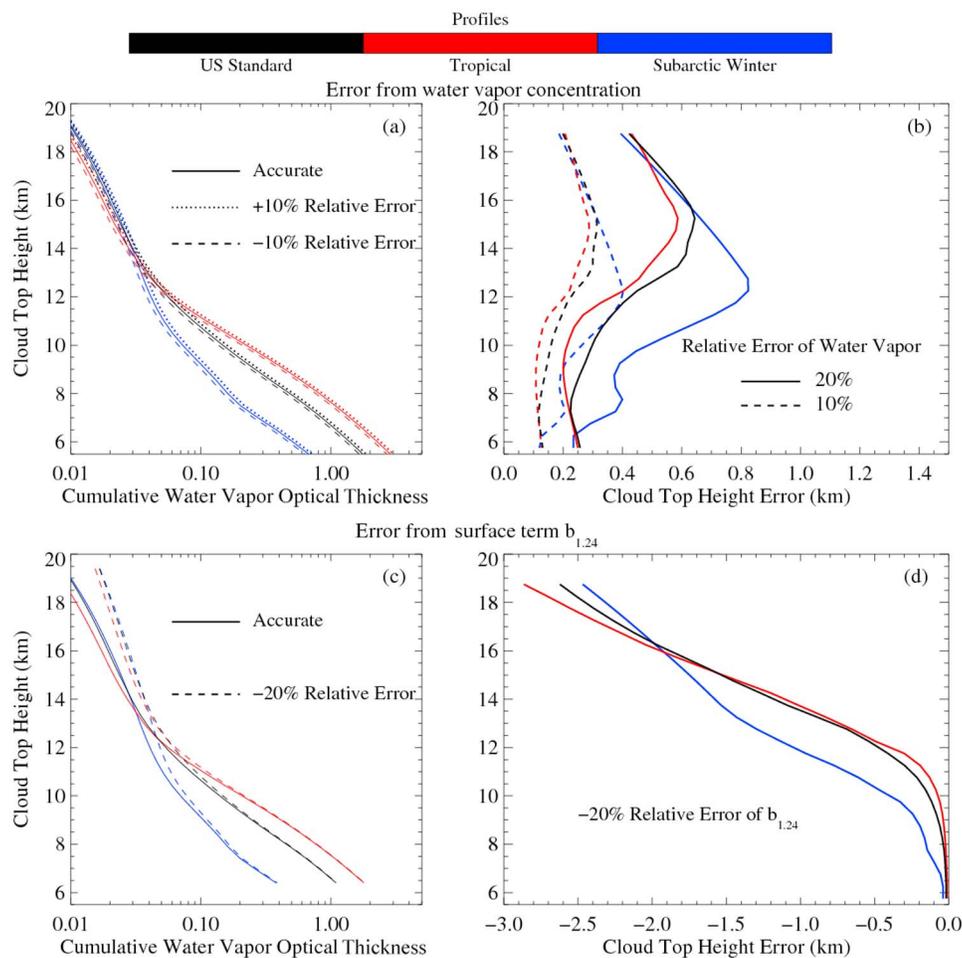

Figure 4. Impact of WV concentration uncertainties on 1.38 CTH retrieval. (a) Cumulative WV optical thickness (1.38-μm) profiles given by US standard (black), tropical (red), and subarctic winter (blue) profiles with/without WV amount uncertainties. (b) Corresponding errors of 1.38 CTH retrievals as a function of CTH using profiles with WV amount uncertainties. (c) Same as Figure 4a, but the for Cumulative WV optical thickness profiles with/without uncertainties from the surface term $b_{1.24}$. (d) Same as Figure 4b, but for corresponding 1.38 CTH errors with uncertainties from the surface term.

sensitivity of the 1.38 CTH to the WV amount is large in this region. It is interesting to note that for very high cloud (e.g., CTH > 14 km), retrieved CTH errors decrease because, although the WV amount is small, the impact from 10% or 20% WV error is also diminished. Similarly, for moderately high cloud (i.e., CTH < 9 km), the errors in CTH tend to increase again because while large WV amounts provide a large sensitivity in the retrieval, the impact of the absolute WV uncertainty is also enhanced and becomes more significant.

[14] Another uncertainty comes from the approximation of first order surface reflection, as shown in equation (5), which underestimates $b_{1.24}$ and from the error of τ_c. As expected, the uncertainty can be maximized if a cloud is optically thin because of the higher order reflection associated with the surface. By using the DISORT and the Cox-Munk ocean surface bi-directional reflectance model [*Cox and Munk*, 1954], we find that for a cloud with optical thickness 0.3, errors from both the first order approximation and the value of τ_c ($\pm 20\%$ relative error of τ_c is introduced) lead to an approximately -13% relative error of $b_{1.24}$. In this study, we introduce a -20% relative error of $b_{1.24}$ to investigate its impact on the 1.38 CTH retrieval. Figure 4c shows the cumulative WV optical thickness values as a function of the CTH. The underestimation of $b_{1.24}$ increases the cumulative WV optical thickness because $T_{two-way,1.38}$ is decreased according to equation (6). Figure 4d shows that CTH can be underestimated by more than 2 km if the CTH exceeds 16 km. The CTH error rapidly decreases and approaches zero near 11 km since the WV amount increases exponentially. Generally, the 1.38 CTH retrieval performs well for cirrus cloud in the troposphere.

5. Conclusions

[15] A new approach is described here for inferring cloud top height (CTH) by using two nearby SWIR channels (i.e., 1.24- and 1.38-μm). Cloud scattering properties are similar at the two wavelengths, but water vapor is much more strongly absorptive at 1.38-μm. With these two channels, the water vapor column above a cloud can be retrieved, and from that the cloud-top height (CTH) can be calculated. The new method mitigates the impact of cloud optical and microphysical properties on the inference of CTH.

[16] The method is demonstrated here by comparing CTH products from a subset of one CALIPSO track and a MODIS granule. We find that the 1.38 CTH is much closer to the CALIPSO CTH than the MODIS Collection 5 product, even as the cloud properties change significantly. The 1.38 CTH method can be applied to satellite-based instruments, which provide observations in the two channels, such as MODIS and the Visible Infrared Imager Radiometer Suite (VIIRS), and it can serve as a complementary method for accurately inferring CTH, particularly for thin clouds in the upper troposphere.

[17] The error estimation shows that the accuracy of 1.38 CTH depends on the accuracy of WV amount and the assumption adopted for the surface. Specifically, a 20% WV concentration error leads to an error of approximately 0.8 km if the atmosphere is dry. Furthermore, if a cloud is optically thin, the treatment of the surface can have a relatively large impact, perhaps leading to an error of more than 2 km in the CTH if the cloud is higher than 16 km.

[19] The Editor thanks two anonymous reviewers for assistance evaluating this paper.

References

Anderson, G. P., S. A. Clough, F. X. Kneizys, J. H. Chetwynd, and E. P. Shettle (1986), AFGL atmospheric constituent profiles (0–120 km), *Tech. Rep. AFGL-TR-86-0110*, Air Force Geophys. Lab., Hanscom Air Force Base, Mass.

Baum, A. B., W. P. Menzel, R. A. Frey, D. C. Tobin, R. E. Holz, and S. A. Ackerman (2012), MODIS cloud-top property refinements for Collection 6, *J. Appl. Meteorol. Climatol.*, 51, 1145–1163, doi:10.1175/JAMC-D-11-0203.1.

Corti, T., B. P. Luo, Q. Fu, H. Vömel, and T. Peter (2006), The impact of cirrus clouds on tropical troposphere-to-stratosphere transport, *Atmos. Chem. Phys.*, 6, 2539–2547, doi:10.5194/acp-6-2539-2006.

Cox, C., and W. Munk (1954), Measurement of the roughness of the sea surface from photographs of the suns glitter, *J. Opt. Soc. Am.*, 44, 838–850, doi:10.1364/JOSA.44.000838.

Dessler, A. E., and P. Yang (2003), The distribution of tropical thin cirrus clouds inferred from Terra MODIS data, *J. Clim.*, 16, 1241–1247, doi:10.1175/1520-0442(2003)16<1241:TDOTTC>2.0.CO;2.

Gao, B.-C., Y. J. Kaufman, W. Han, R.-R. Li, and W. J. Wiscombe (1998), Correction of thin cirrus path radiance in the 0.4–1.0 μm spectral region using the sensitive 1.375-μm channels to retrieve cirrus cloud reflectances from aircraft and satellite data, *J. Geophys. Res.*, 103, 32,169–32,176, doi:10.1029/98JD02006.

Gao, B.-C., P. Yang, W. Han, R.-R. Li, and W. J. Wiscombe (2002), An algorithm using visible and 1.375-μm channels to retrieve cirrus cloud reflectances from aircraft and satellite data, *IEEE Trans. Geosci. Remote Sens.*, 40, 1659–1668, doi:10.1109/TGRS.2002.802454.

Gao, B.-C., K. Meyer, and P. Yang (2004), A new concept on remote sensing of cirrus optical depth and effective ice particle size using strong water vapor absorption channels near 1.38 and 1.88 μm, *IEEE Trans. Geosci. Remote Sens.*, 42, 1891–1899, doi:10.1109/TGRS.2004.833778.

Garrett, T. J., M. A. Zulauf, and S. K. Krueger (2006), Effects of cirrus near the tropopause on anvil cirrus dynamics, *Geophys. Res. Lett.*, 33, L17804, doi:10.1029/2006GL027071.

Heikes, R., and D. A. Randall (1995), Numerical-integration of the shallow-water equations on a twisted icosahedral grid. 1. Basic design and results of tests, *Mon. Weather Rev.*, 123, 1862–1880, doi:10.1175/1520-0493(1995)123<1862:NIOTSW>2.0.CO;2.

Holz, R. E., S. Ackerman, P. Antonelli, F. Nagle, R. O. Knuteson, M. McGill, D. L. Hlavka, and W. D. Hart (2006), An improvement to the high-spectral-resolution CO_2-slicing cloud-top altitude retrieval, *J. Atmos. Oceanic Technol.*, 23, 653–670, doi:10.1175/JTECH1877.1.

Holz, R. E., S. A. Ackerman, F. W. Nagle, R. A. Frey, S. Dutcher, R. E. Kuehn, M. A. Vaughan, and B. A. Baum (2008), Global Moderate Resolution Imaging Spectroradiometer (MODIS) cloud detection and height evaluation using CALIOP, *J. Geophys. Res.*, 113, D00A19, doi:10.1029/2008JD009837.

Jensen, E. J., O. B. Toon, H. B. Selkirk, J. D. Spinhirne, and M. R. Schoeberl (1996), On the formation and persistence of subvisible cirrus clouds near the tropical tropopause, *J. Geophys. Res.*, 101(D16), 21,361–21,375, doi:10.1029/95JD03575.

Menzel, W. P., W. L. Smith, and T. R. Stewart (1983), Improved cloud motion wind vector and altitude assignment using VAS, *J. Appl. Meteorol.*, 22, 377–384, doi:10.1175/1520-0450(1983)022<0377:ICMWVA>2.0.CO;2.

Menzel, W. P., R. A. Frey, and B. A. Baum (2010), Cloud top properties and cloud phase algorithm theoretical basis document, *MODIS/MOD04 ATBD*, 63 pp., NASA Goddard Space Flight Cent., Greenbelt, Md.

Meyer, K., and S. Platnick (2010), Utilizing the MODIS 1.38 μm channel for cirrus cloud optical thickness retrievals: Algorithm and retrieval uncertainties, *J. Geophys. Res.*, 115, D24209, doi:10.1029/2010JD014872.

Meyer, K., P. Yang, and B.-C. Gao (2004), Optical thickness of tropical cirrus clouds derived from the MODIS 0.66 and 1.38-μm channels, *IEEE Trans. Geosci. Remote Sens.*, 42, 833–841, doi:10.1109/TGRS.2003.818939.

Platnick, S., M. D. King, S. A. Ackerman, W. P. Menzel, B. A. Baum, J. C. Riédi, and R. A. Frey (2003), The MODIS cloud products: Algorithms and examples from Terra, *IEEE Trans. Geosci. Remote Sens.*, 41, 459–473, doi:10.1109/TGRS.2002.808301.

Rienecker, M. M., et al. (2008), The GEOS-5 data assimilation system—Documentation of versions 5.0.1, 5.1.0, and 5.2.0, *NASA Tech. Memo., TM-2008*, 27 pp.

Rosenfield, J. E., D. B. Considine, M. R. Schoeberl, and E. V. Browell (1998), The impact of subvisual cirrus clouds near the tropical tropopause on stratospheric water vapor, *Geophys. Res. Lett.*, 25, 1883–1886, doi:10.1029/98GL01294.

Sassen, K., Z. Wang, and D. Liu (2009), Cirrus clouds and deep convection in the tropics: Insights from CALIPSO and CloudSat, *J. Geophys. Res.*, *114*, D00H06, doi:10.1029/2009JD011916.

Schaaf, C. B., et al. (2002), First operational BRDF, albedo and nadir reflectance products from MODIS, *Remote Sens. Environ.*, *83*, 135–148, doi:10.1016/S0034-4257(02)00091-3.

Smith, W. L., and C. M. R. Platt (1978), Comparison of satellite-deduced cloud heights with indications from radiosonde and ground-based laser measurements, *J. Appl. Meteorol.*, *17*, 1796–1802, doi:10.1175/1520-0450(1978)017<1796:COSDCH>2.0.CO;2.

Stamnes, K., S. C. Tsay, W. Wiscombe, and K. Jayaweera (1988), Numerically stable algorithm for discrete-ordinate-method radiative transfer in multiple scattering and emitting layered media, *Appl. Opt.*, *27*, 2502–2509, doi:10.1364/AO.27.002502.

Tobin, D. C., H. E. Revercomb, C. C. Moeller, and T. S. Pagano (2006), Use of Atmospheric Infrared Sounder high-spectral resolution spectra to assess the calibration of Moderate Resolution Imaging Spectroradiometer on EOS Aqua, *J. Geophys. Res.*, *111*, D09S05, doi:10.1029/2005JD006095.

Wang, T., and A. E. Dessler (2012), Analysis of cirrus in the tropical tropopause layer from CALIPSO and MLS data: A water perspective, *J. Geophys. Res.*, *117*, D04211, doi:10.1029/2011JD016442.

Wylie, D. P., and W. P. Menzel (1999), Eight years of high cloud statistics using HIRS, *J. Clim.*, *12*, 170–184, doi:10.1175/1520-0442-12.1.170.